Article

Trapping H Bound to the Nitrogenase FeMo-Cofactor Active Site during H Evolution: Characterization by ENDOR Spectroscopy

Robert Y. Igarashi, Mikhail Laryukhin, Patricia C. Dos Santos, Hong-In Lee, Dennis R. Dean, Lance C. Seefeldt, and Brian M. Hoffman

J. Am. Chem. Soc., **2005**, 127 (17), 6231-6241• DOI: 10.1021/ja043596p • Publication Date (Web): 06 April 2005

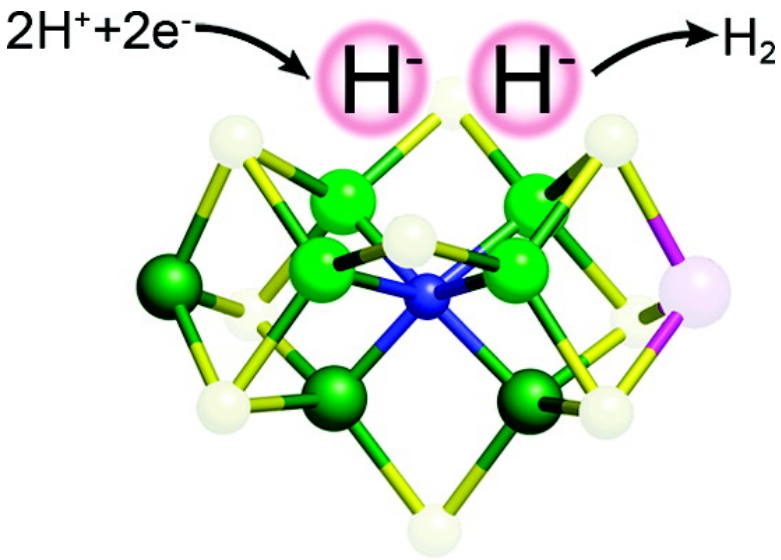

J|A|C|S
ARTICLES
Published on Web 04/06/2005

Trapping H^- Bound to the Nitrogenase FeMo-Cofactor Active Site during H_2 Evolution: Characterization by ENDOR Spectroscopy

Robert Y. Igarashi,[†] Mikhail Laryukhin,[‡] Patricia C. Dos Santos,[§] Hong-In Lee,[||] Dennis R. Dean,*[,§] Lance C. Seefeldt,*[,†] and Brian M. Hoffman*[,‡]

Contribution from the Department of Chemistry and Biochemistry, Utah State University, Logan, Utah 84322, Department of Chemistry, Northwestern University, Evanston, Illinois 60208, Department of Biochemistry, Virginia Tech, Blacksburg, Virginia 24061, and Department of Chemistry Education, Kyungpook National University, Daegu 702-701, Korea

Received October 21, 2004; E-mail: bmh@northwestern.edu; deandr@vt.edu; seefeldt@cc.usu.edu.

Abstract: We here show that the iron−molybdenum (FeMo)-cofactor of the nitrogenase α-70^{Ile} molybdenum−iron (MoFe) protein variant accumulates a novel $S = {}^1/_2$ state that can be trapped during the reduction of protons to H_2. ^{1,2}H-ENDOR measurements disclose the presence of two protons/hydrides ($H^{+/-}$) whose hyperfine tensors have been determined from two-dimensional field-frequency ^{1}H ENDOR plots. The two $H^{+/-}$ have large isotropic hyperfine couplings, $A_{iso} \approx 23$ MHz, which shows they are bound to the cofactor. The favored analysis for these plots indicates that the two $H^{+/-}$ have the same principal values, which indicates that they are chemically equivalent. The tensors are further related to each other by a permutation of the tensor components, which indicates an underlying symmetry of binding relative to the cofactor. At present, no model for the structure of the iron−molybdenum (FeMo)-cofactor in the $S = {}^1/_2$ state trapped during the reduction of H^+ can be shown unequivocally to satisfy all of the constraints generated by the ENDOR analysis. The data disfavors any model that involves protonation of sulfides, and thus suggests that the intermediate instead contains two chemically equivalent bound hydrides; it appears unlikely that these are terminal monohydrides.

Nitrogenase is the metalloenzyme responsible for biological nitrogen fixation, catalyzing ammonia production with the ideal stoichiometry of eq 1.[1]

$$N_2 + 8\,e^- + 16\,MgATP + 8\,H^+ \rightarrow 2\,NH_3 + H_2 + 16\,MgADP + 16\,P_i \quad (1)$$

The molybdenum-dependent nitrogenases represent the most widely distributed and best-studied class of these enzymes and comprise two component proteins called the iron (Fe) protein and the molybdenum−iron (MoFe) protein. The Fe protein delivers electrons to the MoFe protein in a reaction that is coupled to the hydrolysis of two equivalents of MgATP for each electron transferred.[2−5] The MoFe protein contains [8Fe-7S] (P) cluster that accepts electrons from the Fe protein and subsequently transfers electrons to the active site-metal cluster iron−molybdenum (FeMo)-cofactor [7Fe-9S-Mo-X-homocitrate],[6,7] where X is an atom of unknown identity but proposed to be a N.[8] In addition to reducing the physiological substrates N_2 and H^+, nitrogenase also reduces a range of small compounds having double or triple bonds, such as acetylene ($HC{\equiv}CH \rightarrow H_2C{=}CH_2$) by multiples of two electrons and two protons.[1,9,10]

The fundamental question about nitrogenase function remains unanswered: where do H^+ and N_2 bind, and what is the mechanism for H_2 and NH_3 formation.[11] The Mo atom has been suggested to provide a substrate binding site, and its involvement is supported by theoretical calculations on FeMo-cofactor fragments[12,13] and reactivity studies with inorganic model compounds, outside of a protein.[14−16] Alternatively, one (or

[†] Utah State University.
[‡] Northwestern University.
[§] Virginia Tech.
[||] Kyungpook National University.

(1) Burgess, B. K.; Lowe, D. J. *Chem. Rev.* **1996**, *96*, 2983−3012.
(2) Hageman, R. V.; Orme-Johnson, W. H.; Burris, R. H. *Biochemistry* **1980**, *19*, 2333−2342.
(3) Thorneley, R. N.; Eady, R. R.; Yates, M. G. *Biochim. Biophys. Acta* **1975**, *403*, 269−284.
(4) Seefeldt, L. C.; Dean, D. R. *Acc. Chem. Res.* **1997**, *30*, 260−266.
(5) Howard, J. B.; Rees, D. C. *Annu. Rev. Biochem.* **1994**, *63*, 235−264.
(6) Howard, J. B.; Rees, D. C. *Chem. Rev.* **1996**, *96*, 2965−2982.
(7) Rees, D. C.; Howard, J. B. *Curr. Opin. Chem. Biol.* **2000**, *4*, 559−566.
(8) Einsle, O.; Texcan, F. A.; Andrade, S. L. A.; Schmid, B.; Yoshida, M.; Howard, J. B.; Rees, D. C. *Science* **2002**, *297*, 1696−1700.
(9) Igarashi, R. Y.; Seefeldt, L. C. *Crit. Rev. Biochem. Mol. Biol.* **2003**, *38*, 351−384.
(10) Dilworth, M. J. *Biochim. Biophys. Acta* **1966**, *127*, 285−294.
(11) Seefeldt, L. C.; Dance, I. G.; Dean, D. R. *Biochemistry* **2004**, *43*, 1401−1409.
(12) Durrant, M. C. *Inorg. Chem. Commun.* **2001**, *4*, 60−62.
(13) Durrant, M. C. *Biochemistry* **2002**, *41*, 13934−13945.
(14) Liu, H., I.; Filipponi, A.; Gavini, N.; Burgess, B. K.; Hedman, B.; Di Cicco, A.; Natoli, C. R.; Hodgson, K. O. *J. Am. Chem. Soc.* **1994**, *116*, 2418−2423.
(15) Malinak, S. M.; Coucouvanis, D. In *Progress in Inorganic Chemistry*; Karlin, K. D., Ed.; Wiley: New York, 2001; Vol. 49, pp 599−662.
(16) Yandulov, D. V.; Schrock, R. R. *Science* **2003**, *301*, 76−78.

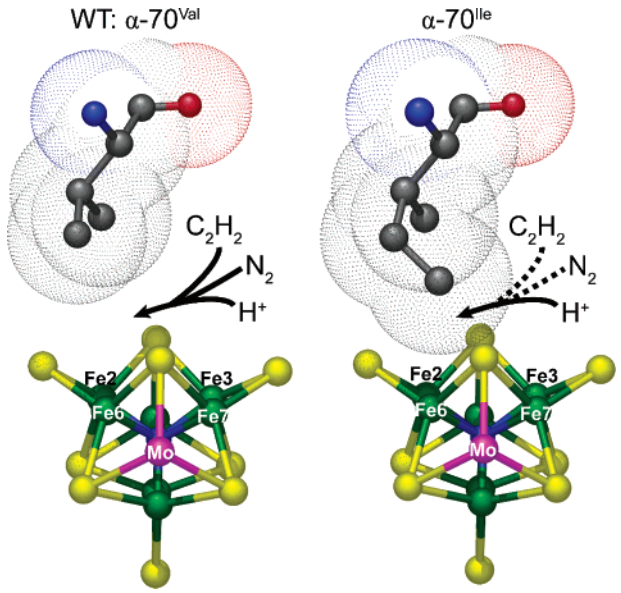

Figure 1. Proposed constraints on substrate binding at the nitrogenase active site. Shown is FeMo-cofactor (looking down from the Mo end with homocitrate removed) and the side chain of α-70^{Val} (wild-type, PDB file 1M1N on left) or α-70^{Ile} (on right) with dots added to show the van der Waals surfaces for these amino acids. The arrows convey the relative reduction activities for H^+, N_2 and C_2H_2 as substrates, with solid arrows indicating high rates of reduction and dashed arrows indicating diminished rates of reduction. The figure was generated with the program PyMOL and the color scheme is Fe in green, S in yellow, C in gray, N in blue, and the Mo in magenta. The atom of unknown identity in the center of FeMo-cofactor is shown in blue.

more) of the six Fe atoms that comprise the waist section of FeMo-cofactor could bind substrate.[17−23] These six Fe atoms are contained in three symmetrically (C_3) related [4Fe-4S] faces, each of which might provide a location for substrate binding and reduction.

We have presented evidence that alkyne substrates, such as propargyl alcohol, ($HC{\equiv}CCH_2OH$), bind to one [4Fe-4S] face of FeMo-cofactor composed of Fe atoms 2, 3, 6, and 7. This face of the FeMo-cofactor is approached by a Val-residue at position 70 of the α-subunit (Figure 1). Substitution of this residue by amino acids with smaller side chains, like Ala, results in a MoFe protein that is able to reduce larger alkynes, including propyne ($HC{\equiv}CCH_3$) to propene ($H_2C{=}CHCH_3$) and propargyl alcohol to allyl alcohol ($H_2C{=}CCH_2OH$).[24] A reasonable conclusion from these results is that these substrates bind to the FeS face approached by α-70^{Val}. An intermediate state with the FeMo-cofactor in an $S = {}^1/_2$ state was freeze-trapped during propargyl alcohol reduction. Characterization by electron paramagnetic resonance (EPR) and electron nuclear double resonance (ENDOR) spectroscopies[18,25] definitively assigned the cluster of the intermediate as binding the allyl alcohol reduction

Scheme 1

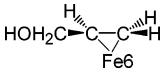

product as a ferracyclopropane (Scheme 1). This assignment was subsequently confirmed by studies of the pH dependence of the reaction[26] and DFT computations,[19] which further identified as the binding site, Fe6 of the cofactor FeS face approached by α-70^{Val}. It is reasonable to extend the binding site and mode of binding found with propargyl alcohol to the binding of other alkynes.

More recently, we found that increasing the size of the side chain at position α-70, through substitution of α-70^{Val} by Ile, significantly restricts both the reduction of alkyne substrates, including acetylene, and the reduction of N_2.[27] As the α-70^{Ile} MoFe protein retains full proton reduction activity, this restriction does not reflect perturbations of cluster reactivity or of electron delivery; instead these observations suggest that N_2 and alkynes both bind to the FeS face composed of Fe atoms 2, 3, 6, and 7 (Figure 1). We here report that the FeMo-cofactor of the α-70^{Ile} MoFe protein converts to an $S = {}^1/_2$, EPR-active state during H^+ reduction/H_2 evolution. This intermediate state has been freeze-trapped and characterized by ^{1,2}H ENDOR spectroscopy. These measurements show that the cofactor of this state covalently binds two chemically equivalent $H^{+/-}$, and give the first experimental insights into the structure of an intermediate formed during H_2 evolution catalyzed by nitrogenase.

Experimental Procedures

Protein Purification and Activity Assays. An *Azotobacter vinelandii* strain (DJ1373) expressing the α-70^{Ile} variant MoFe protein was constructed using a site-directed mutagenesis and gene replacement protocol as previously described.[28] The wild-type and α-70^{Ile} variant MoFe proteins were purified using a poly-His metal affinity chromatography system described earlier.[29] The wild-type Fe protein component of nitrogenase was purified essentially as previously described.[30] All manipulations of proteins were conducted in septum-sealed serum vials under an argon atmosphere, and all anaerobic liquid and gas transfers were performed using gastight syringes. Acetylene reduction and H_2 evolution activities were determined as described earlier.[31,32] NH_3 formation from the reduction of N_2 was quantified using a liquid chromatographic−fluorescence method with *o*-phthalaldehyde mercaptoethanol as previously described.[26,33]

Preparation of Nonturnover and Turnover MoFe Proteins Samples for EPR. Resting-state MoFe protein (100 μM) samples were made in 100 mM MOPS buffer (pH 7.0) with 30 mM sodium dithionite ($Na_2S_2O_4$) under 1 atm of Ar. Nitrogenase turns over and reduces protons when electrons are supplied in the absence of other substrates. Nitrogenase turnover samples were prepared by the addition of the Fe

(17) Dance, I. G. *Aust. J. Chem.* **1994**, *47*, 979−990.
(18) Lee, H. I.; Igarashi, R. Y.; Laryukhin, M.; Doan, P. E.; Dos Santos, P. C.; Dean, D. R.; Seefeldt, L. C.; Hoffman, B. M. *J. Am. Chem. Soc.* **2004**, *126*, 9563−9569.
(19) Dance, I. *J. Am. Chem. Soc.* **2004**, *126*, 11852−11863.
(20) Betley, T. A.; Peters, J. C. *J. Am. Chem. Soc.* **2004**, *126*, 6252−6254.
(21) Smith, J. M.; Lachicotte, R. J.; Holland, P. L. *J. Am. Chem. Soc.* **2003**, *125*, 15752−15753.
(22) Smith, J. M.; Lachicotte, R. J.; Pittard, K. A.; Cundari, T. R.; Lukat-Rodgers, G.; Rodgers, K. R.; Holland, P. L. *J. Am. Chem. Soc.* **2001**, *123*, 9222−9223.
(23) Vela, J.; Stoian, S.; Flaschenriem, C. J.; Munck, E.; Holland, P. L. *J. Am. Chem. Soc.* **2004**, *126*, 4522−4523.
(24) Mayer, S. M.; Niehaus, W. G.; Dean, D. R. *J. Chem. Soc., Dalton Trans.* **2002**, *2002*, 802−807.
(25) Benton, P. M.; Laryukhin, M.; Mayer, S. M.; Hoffman, B. M.; Dean, D. R.; Seefeldt, L. C. *Biochemistry* **2003**, *42*, 9102−9109.
(26) Igarashi, R. Y.; Dos Santos, P. C.; Niehaus, W. G.; Dance, I. G.; Dean, D. R.; Seefeldt, L. C. *J. Biol. Chem.* **2004**, *279*, 34770−34775.
(27) Barney, B. M.; Igarashi, R. Y.; Dos Santos, P. C.; Dean, D. R.; Seefeldt, L. C. *J. Biol. Chem.* **2004**. In press.
(28) Christiansen, J.; Cash, V. L.; Seefeldt, L. C.; Dean, D. R. *J. Biol. Chem.* **2000**, *275*, 11459−11464.
(29) Christiansen, J.; Goodwin, P. J.; Lanzilotta, W. N.; Seefeldt, L. C.; Dean, D. R. *Biochemistry* **1998**, *37*, 12611−12623.
(30) Burgess, B. K.; Jacobs, D. B.; Stiefel, E. I. *Biochim. Biophys. Acta* **1980**, *614*, 196−209.
(31) Seefeldt, L. C.; Morgan, T. V.; Dean, D. R.; Mortenson, L. E. *J. Biol. Chem.* **1992**, *267*, 6680−6688.
(32) Seefeldt, L. C.; Rasche, M. E.; Ensign, S. A. *Biochemistry* **1995**, *34*, 5382−5389.
(33) Corbin, J. L. *App. Environ. Microbiol.* **1984**, *47*, 1027−1030.

protein (50 μM) to an anaerobic vial containing a solution of the MoFe protein (100 μM) in 100 mM MOPS buffer (pH 7.0) containing 30 mM sodium dithionite, 10 mM ATP, 15 mM $MgCl_2$, 20 mM phosphocreatine, 2 mg/mL bovine serum albumin, and 0.3 mg/mL creatine phosphokinase. Catalytic proton reduction was allowed to continue for ca. 20 s at room temperature, and then the sample was placed in a standardized 4-mm quartz EPR tubes and quenched by freezing in liquid N_2.

Preparation of Turnover MoFe Proteins for ENDOR. Turnover samples of the α-70^{Ile} MoFe protein (150 μM) were prepared in 100 mM MOPS buffer (pH 7.0, containing 5 mM ATP, 7.5 mM $MgCl_2$, 30 mM phosphocreatine, 30 mM dithionite, 2 mg/mL BSA, and 0.3 mg/mL creatine phophokinase) and 75 μM Fe protein. The reaction was allowed to progress at room temperature (ca. 23 °C) for ca. 20 s and was quenched by freezing in liquid N_2. Samples in D_2O were prepared similarly, except that all reaction components were made in MOPS/D_2O buffer and the α-70^{Ile} MoFe protein was exchanged into 100 mM MOPS buffer (pH 7.0) containing 250 mM NaCl made in D_2O with pH adjustment using NaOD. These samples contained <7% protic solvent resulting from carry over from the addition of the Fe protein solution.

X-Band EPR Spectroscopy. X-band EPR spectra were recorded on a Bruker ESP-300E spectrometer equipped with an ER 4116 dual-mode X-band cavity including an Oxford Instruments ESR-900 helium flow cryostat. EPR spectra were recorded at a modulation frequency of 100 kHz, a modulation amplitude of 1.26 mT (12.6 G), a sweep rate of 10 mT/s, and a microwave frequency of approximately 9.65 GHz (with the precise value recorded for each spectrum to ensure exact *g* alignment). All spectra were recorded at 8 K and a microwave power of 2.0 mW, with each trace being the sum of five scans, unless stated otherwise in figure legends. The program IGOR Pro (WaveMetrics, Lake Oswego, OR) was used for all subsequent manipulation of spectral data.

ENDOR Spectroscopy. Q band (35GHz) cw EPR and ENDOR spectra were recorded on a modified Varian E−110 spectrometer equipped with a helium immersion dewar at 2 K under "rapid passage" condition using 100-kHz field modulation.[34] Q-band Mims three-pulse ENDOR spectra, pulse sequence, $t_{mw}-\tau-t_{mw}-T(\mathrm{rf})-t_{mw}-\tau$-echo,[35] were obtained at 2 K on a locally constructed spectrometer.[36]

In first order, the ^{1}H ENDOR spectrum of a proton coupled to an $S = {}^1/_2$ spin center (single orientation) is a doublet with frequencies given by

$$\nu_{\pm} = |\nu_H \pm A/2| \qquad (2)$$

Here, ν_H is the proton Larmor frequency and A is the orientation-dependent hyperfine coupling constant of the coupled nucleus. Complete nuclear hyperfine tensors are derived from frozen-solution samples through simulation of two-dimensional (2D) field-frequency plots composed of multiple ENDOR spectra taken across the EPR envelope of the paramagnetic species under study, following published procedures.[37−40] The hyperfine tensor is defined by the principal tensor components, $[A_1, A_2, A_3]$, and the relative orientation of the tensor-frame with respect to *g*-frame, defined by Euler angles, $[\varphi, \theta, \psi]$.[41]

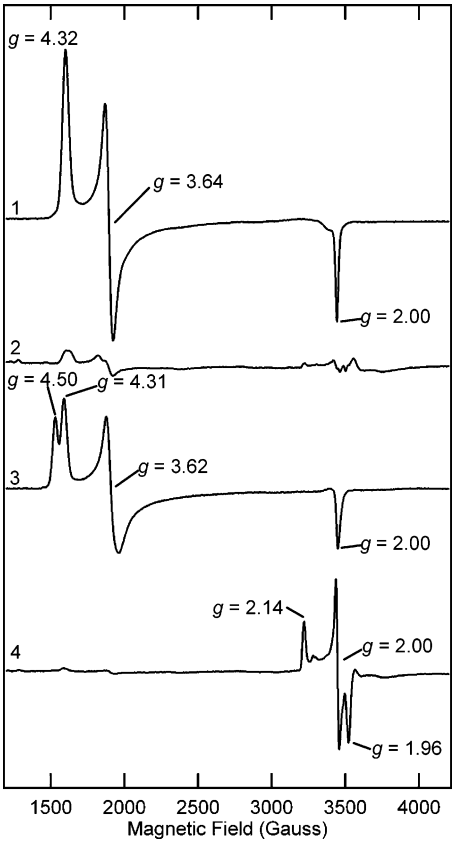

Figure 2. EPR spectra of wild-type and α-70^{Ile} MoFe proteins in the resting and turnover states. Resting state EPR spectra are shown for the wild-type (trace 1) and α-70^{Ile} (trace 3) MoFe proteins. Also shown are spectra for turnover states during H_2 evolution for the wild-type (trace 2) and α-70^{Ile} (trace 4) MoFe proteins. Numbers noted near the inflections are *g* values for the EPR absorption peaks. All samples contained 100 μM MoFe and are scaled the same. Other conditions are presented in the Experimental Procedures section.

Results

EPR Characterization of the Resting and Turnover States of the α-70^{Ile} MoFe Protein. The dithionite-reduced, resting state of FeMo-cofactor in the wild-type MoFe protein exhibits a rhombic $S = {}^3/_2$ EPR spectrum with *g* values of 4.32, 3.64, and 2.00 (Figure 2, trace 1).[42] The resting state of the α-70^{Ile} MoFe protein shows two overlapping $S = {}^3/_2$ EPR signals from the FeMo-cofactor, with slight differences in the rhombicity of their **g** tensors (Figure 2, trace 3). As expected, the power-saturation and temperature dependences of the resting-state FeMo-cofactor signal are indistinguishable for the resting states of the wild-type and α-70^{Ile} MoFe proteins, with the signal intensities displaying a Curie-law-dependent decrease with increasing temperature from 4 K, Figure 3.

When the wild-type MoFe protein is trapped during turnover under Ar (H^+ reduction), this EPR signal is observed to diminish in intensity, consistent with the conversion to a more reduced, EPR-silent state (Figure 2, trace 2).[43,44] When the α-70^{Ile} MoFe protein is trapped during turnover under Ar (H^+ reduction), the resting-state FeMo-cofactor EPR signal is instead changed to a

(34) Werst, M. M.; Davoust, C. E.; Hoffman, B. M. *J. Am. Chem. Soc.* **1991**, *113*, 1533−1538.
(35) Schweiger, A.; Jeschke, G. *Principles of Pulse Electron Paramagnetic Resonance*; Oxford University Press: Oxford, UK, 2001.
(36) Davoust, C. E.; Doan, P. E.; Hoffman, B. M. *J. Magn. Reson.* **1996**, *119*, 38−44.
(37) Hoffman, B. M.; Martinsen, J.; Venters, R. A. *J. Magn. Reson.* **1984**, *59*, 110−123.
(38) Hoffman, B. M.; Venters, R. A.; Martinsen, J. *J. Magn. Reson.* **1985**, *62*, 537−542.
(39) Hoffman, B. M.; DeRose, V. J.; Doan, P. E.; Gurbiel, R. J.; Houseman, A. L. P.; Telser, J. *Biol. Magn. Reson.* **1993**, *13*, 151−218.
(40) Doan, P. E. In *Paramagnetic Resonance of Metallobiomolecules*; Telser, J., Ed.; American Chemical Society: Washington, DC, 2003; pp 55−81.
(41) Mathews, J.; Walker, R. L. *Mathematical Methods of Physics*; W. A. Benjamin, Inc.: New York, 1965.
(42) Orme-Johnson, W. H.; Hamilton, W. D.; Jones, T. L.; Tso, M. Y.; Burris, R. H.; Shah, V. K.; Brill, W. J. *Proc. Natl. Acad. Sci. U.S.A.* **1972**, *69*, 3142−3145.
(43) Huynh, B. H.; Henzl, M. T.; Christner, M. T.; Zimmerman, R.; Orme-Johnson, W. H.; Münck, E. *Biochim. Biophys. Acta* **1980**, *623*, 124−138.
(44) Yoo, S. J.; Angove, H. C.; Papaefthymiou, V.; Burgess, B. K.; Münck, E. *J. Am. Chem. Soc.* **2000**, *122*, 4926−4936.

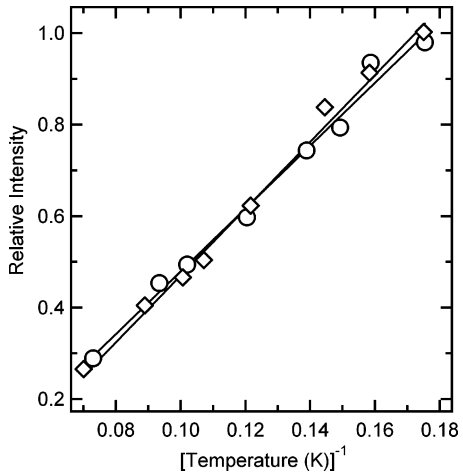

Figure 3. Temperature dependence of EPR signals for the α-70^{Ile} MoFe protein. EPR signal intensities at temperatures from 5.6 to 14 K for the $S = {}^1/_2$ turnover intermediate ($g = 2.14$ inflection, ○) and for the resting state ($g = 4.50$ inflection, ◇). The peak intensities, relative to the maximal intensities, are plotted against inverse temperature (K). *Conditions:* Microwave power, 20 μW for the turnover sample and 500 μW for the resting-state sample; all other parameters were as described in the Experimental Procedures.

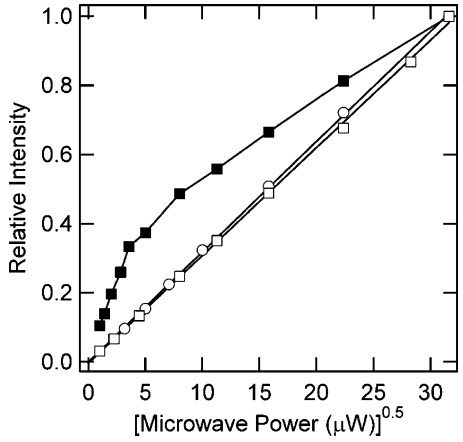

Figure 4. Microwave power dependence of the EPR signals for wild-type and α-70^{Ile} MoFe proteins. EPR signal intensities were determined at a constant temperature of 5.6 K at microwave powers ranging from 0.021 to 1 mW for the $g = 4.50$ inflection of the α-70^{Ile} MoFe protein under nonturnover conditions (□), for the $g = 4.32$ inflection of the wild-type MoFe protein under nonturnover conditions (○), and for the $g = 2.14$ inflection of the α-70^{Ile} MoFe protein under turnover conditions with protons as substrate (■). The peak intensities, relative to the maximal intensities, are plotted against the square root of the microwave power (μW). *Conditions:* See Experimental Procedures.

novel $S = {}^1/_2$ rhombic EPR signal with g values, (g_1, g_2, g_3) = (2.14, 2.00, 1.96) (Figure 2, trace 4). Smaller inflections at $g =$ 2.07 and in the $g \approx 1.93-1.90$ region arise from the [4Fe-4S]$^{1+}$ cluster of the Fe protein.

The temperature and power dependence of the EPR signal for this new state are shown in Figures 3 and 4, respectively. This signal decreases in intensity with increasing temperature in a Curie-like fashion (Figure 3). The $S = {}^1/_2$ intermediate saturates at much lower microwave power than the $S = {}^3/_2$ resting state, as shown by the nonlinear dependence of the relative peak height on the square root of the applied microwave power for the former, as compared to the linear power dependence of the $S = {}^3/_2$ resting states of both the wild-type and α-70^{Ile} MoFe proteins (Figure 4). The properties of the trapped proton turnover state are similar to those of the trapped

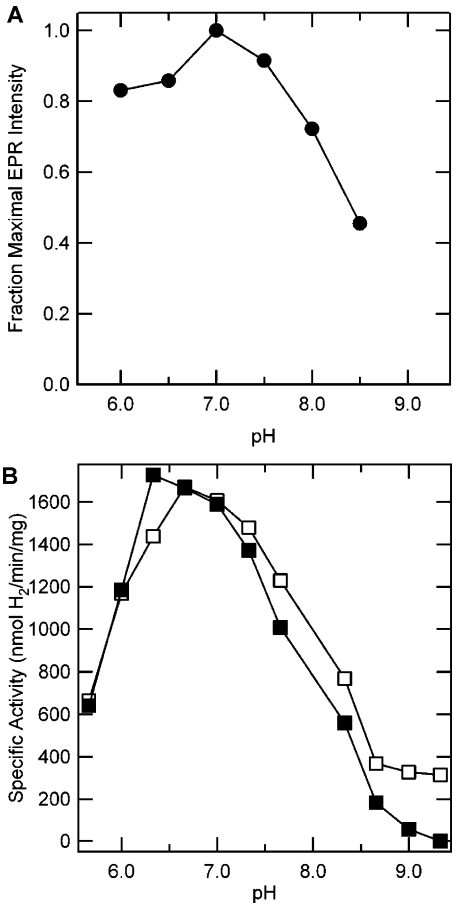

Figure 5. pH dependences for proton interaction with the α-70^{Ile} MoFe protein. (Panel A) The pH dependence of the α-70^{Ile} proton turnover EPR signal ($g = 2.14$) intensity is shown (●). (Panel B) The pH dependence on the specific activity of proton reduction activity is shown for the wild-type (□) and the α-70^{Ile} (■) MoFe proteins. Reaction conditions for both the EPR samples and H^+ reduction activity assays are specified in Experimental Procedures.

allyl alcohol adduct.[25] As the g values and saturation behavior appear to be characteristic of intermediates in which a substrate/product/inhibitor is bound to the FeMo-cofactor,[25,45−48] it suggests that one or more protons/hydrides ($H^{+/-}$) may be bound in the turnover α-70^{Ile} MoFe protein.

pH Dependence of Proton Reduction. Given that protons are the only available substrate for the formation of the EPR-detectable intermediate observed here, the effect of pH on the formation of its EPR signal was examined. The pH dependence of the H^+ turnover EPR signal from the α-70^{Ile} MoFe protein mirrors the pH dependence for proton reduction activity in both the wild-type and α-70^{Ile} MoFe proteins (Figure 5, panel B), with maximal intensity at pH 7.0 (Figure 5, panel A). Interestingly, the α-70^{Ile} MoFe protein shows a slightly more pronounced decline in proton reduction activity with increasing pH when compared to the wild-type MoFe protein. Overall, however, the similarity in the pH profiles is compatible with similar mechanisms for H^+ reduction in mutant and wild-type enzyme.

(45) Ryle, M. J.; Lee, H. I.; Seefeldt, L. C.; Hoffman, B. M. *Biochemistry* **2000**, *39*, 1114−1119.
(46) Hwang, J. C.; Chen, C. H.; Burris, R. H. *Biochim. Biophys. Acta* **1973**, *292*, 256−270.
(47) Davis, L. C.; Henzl, M. T.; Burris, R. H.; Orme-Johnson, W. H. *Biochemistry* **1979**, *18*, 4860−4869.
(48) Sorlie, M.; Christiansen, J.; Dean, D. R.; Hales, B. J. *J. Am. Chem. Soc.* **1999**, *121*, 9457−9458.

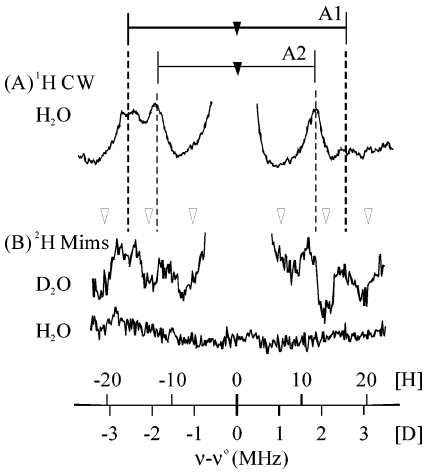

Figure 6. Q-band $^{1/2}$H ENDOR at ~g_3 (=1.96) of the α-70^{Ile} MoFe protein turnover intermediate. (A) cw ENDOR of the intermediate in H_2O buffer and (B) Mims ENDOR of the intermediate in H_2O/D_2O buffer. Open triangles indicate the frequencies of Mims holes. *Experimental Conditions:* (A) Microwave frequency, 35.139 GHz; modulation amplitude, 1.3 G; rf scan speed, 1.5 MHz/s; temperature, 2 K; the bandwidth of the rf excitation was broadened to 60 kHz. (B) Microwave frequency, 34.85 GHz; microwave pulse width, 52 ns; $\tau = 480$ ns; rf pulse width, 30 ms; repetition rate, 50 Hz; temperature, 2 K.

ENDOR Spectroscopy. Figure 6 A and Figure 7 (bottom spectrum) show single-crystal-like Q-band ^{1}H cw ENDOR spectrum obtained near $g_3 = 1.96$ of the α-70^{Ile} MoFe protein $S = {}^1/_2$ turnover intermediate; the top spectrum of Figure 7 shows the single-crystal-like spectrum near $g_1 = 2.14$. Both spectra reveal two resolved ^{1}H doublets with remarkably large hyperfine couplings: $A1(g_3) = 33$ MHz, $A2(g_3) = 25$ MHz. Such large hyperfine interactions of ^{1}H coupled to the cofactor spin are unprecedented and require that the two protons/hydrides ($H^{+/-}$) are bound directly to the FeMo-cofactor; this is confirmed by the presence of a large isotropic hyperfine coupling for both (vide infra). For comparison, the *largest* couplings to the protons of the allyl alcohol bound to the cofactor in the intermediate formed during turnover of the α-70^{Ala} MoFe protein with propargyl alcohol, which itself is quite large, is $A_{max} = 22.5$ MHz,[18] and the *largest* couplings to the protons of the acetylene bound to the cofactor in the turnover state of the α-195^{Gln} MoFe protein is only $A_{max} \approx 18$ MHz.[49] When the α-70^{Ile} MoFe protein is turned over in D_2O buffer, the two corresponding ^{2}H signals appear, indicating that the two resolved ^{1}H doublets are solvent-exchangeable and indeed arise from two bound $H^{+/-}$ (Figure 6 B).

To determine the full hyperfine tensors for the two $H^{+/-}$, we generated a 2D field-frequency ENDOR pattern comprising numerous spectra collected across the EPR envelope (Figure 7). The two ^{1}H signals are quite distinct near both the g_1 and g_3 single-crystal positions, but they split and overlap substantially at intermediate fields. As a consequence of this complicated 2D pattern, we must consider two different interpretations, which differ in how one assigns the signals at g_1 and g_3.

In scenario "A", the patterns of ^{1}H1 and ^{1}H2 'cross' at intermediate fields, such that $A1(g_1) < A2(g_1)$ but $A1(g_3) > A2(g_3)$ (Figure 7). In this scenario, a very successful simulation of the 2D pattern is obtained as the overlap of signals with hyperfine

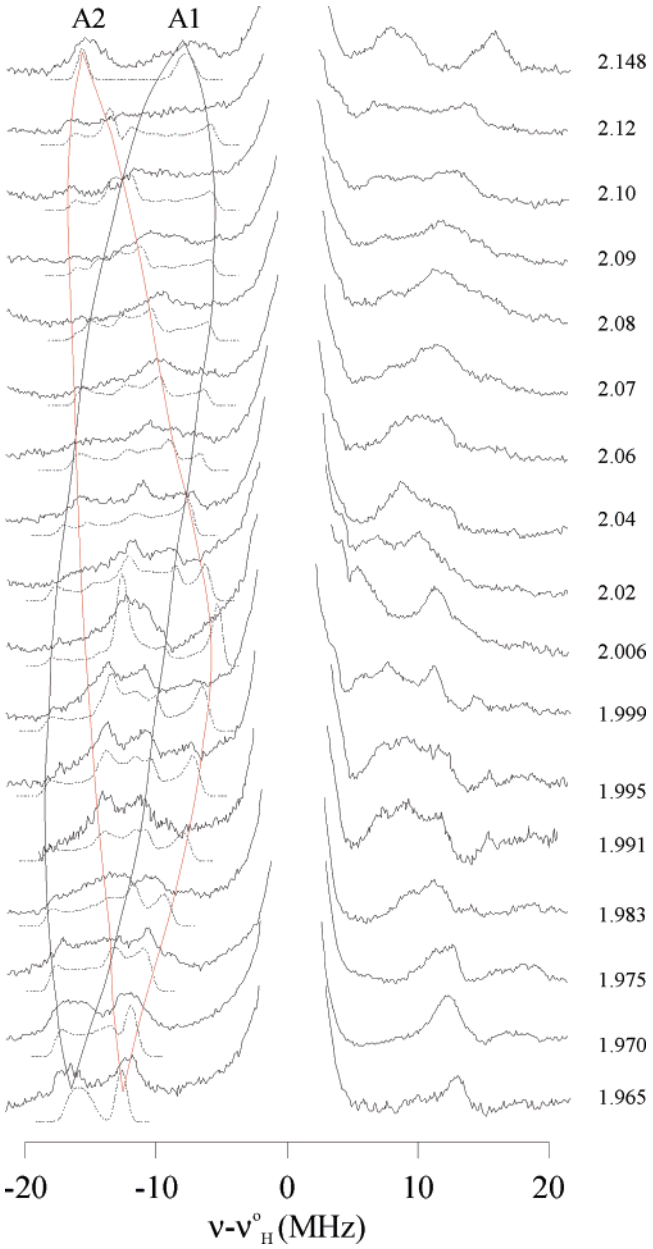

Figure 7. Q-band ^{1}H CW ENDOR of the α-70^{Ile} MoFe protein turnover intermediate. Experimental data (—) and numerical simulation for scenario A (···). Simulation parameters are listed in Table 1. Only ν_- branch (eq 2) of a simulated spectrum is displayed because nuclear relaxation effects distort features of the ν_+ branch. Curves connecting spectra at different g-values are added to guide the eye through the 2D plot. *Experimental Conditions:* same as in Figure 6 A.

tensors that have essentially the same principal values for ^{1}H1 and ^{1}H2 (Table 1); Figure 7 superimposes the experimental spectra with calculated sums of simulations with these two tensors.

The implication of equal principal values can be recognized by recalling that the hyperfine coupling tensor, **A**, for a nucleus associated with a multinuclear spin-coupled cluster can be written as a sum over the nuclear interactions with the electron spins of the individual ions in the absence of spin coupling, A_i, as weighted by the vector-coupling coefficients of the ions (K_i);[50,51]

$$\mathbf{A} = \sum K_i A_i; \quad \sum K_i = 1 \tag{3}$$

We suggest it would require a fortuitous circumstance to find

(49) Lee, H.-I.; Sorlie, M.; Christiansen, J.; Song, R.; Dean, D. R.; Hales, B. J.; Hoffman, B. M. *J. Am. Chem. Soc.* **2000**, *122*, 5582−5587.

Table 1. ^{1}H Hyperfine Tensors of Proton/Hydride Bound to the α-70^{Ile} FeMo-Cofactor during Turnover

scenario[a]	^{1}H	hyperfine tensor[b] (MHz)	A_{iso} (MHz)	**T** (MHz)	Euler angles (deg)
A	^{1}H1	11(1), 25(2), 37(1)	24.3	−13.3, 0.7, 12.7	0, 25, 10
	^{1}H2	33(1), 10(1), 24(2)	22.3	10.7, −12.3, 1.7	0, 25, 0
B	^{1}H1	33(1), 6(2), 35(1)	24.7	8.3, −18.6, 10.3	0, 25, 25
	^{1}H2	11(2), 24(2), 30(2)	21.7	−10.7, 2.3, 8.3	0, 35, 0

[a] Two possible interpretations of ^{1}H ENDOR. Scenario A better describes the observed data than senario B. [b] Hyperfine tensor = A_{iso}**1**+ **T** (**1** is unit matrix). The relative signs of components is fixed by the simulations, but the absolute signs of the hyperfine couplings are not determined; thus, we have let the signs of the hyperfine tensors be positive.

the same tensor sum for **A** of two different types of $^1H^{+/-}$. Hence we infer that H1 and H2 are bound in a *chemically equivalent* manner.

The two ^{1}H tensors both have large isotropic and anisotropic contributions, summed to give a distinctive form for **A**: when the principal values are arranged in increasing magnitude, one sees that $\mathbf{A} \approx [a, 2a, 3a]$, where $a \approx 10-11$ MHz. As a result, the tensors can be decomposed into the sum of a large isotropic coupling, $A_{iso} = 24.3$, 22.3 MHz for H1 and H2, respectively, plus a large and almost completely rhombic anisotropic term, $\mathbf{T} \approx [-t, 0, t]$, where $t \approx 10-12$ MHz, Table 1.

Although ^{1}H1 and ^{1}H2 have the same principal values and thus presumably have equivalent bonds to the cofactor, their hyperfine tensors are oriented differently relative to the **g** tensor. It is important to emphasize that the relative orientations of the two, otherwise equivalent, tensors are unusually well defined in the present study.

In the simplest analysis, the tensors are coaxial (Figure S1 A), (Euler angles with respect to *g*-frame of [$\varphi = 0°$, $\theta = 25°$ $\psi = 10°$]) but with their principal values permuted: ($A_1 \leftarrow A_2 \leftarrow A_3 \leftarrow A_1$). Given the numerous elements of three-fold symmetry displayed by the cofactor, it is perhaps useful to recognize that one way for such a permutation to occur would be if the two ^{1}H were related by a 120° rotation about a trigonal axis through a face of an octahedron, as illustrated in Figure S1 C and Figure 10A (below). Because of a degeneracy in the correspondence between ENDOR frequencies and the molecular orientation relative to the external field, the analysis in fact allows H1 and H2 to have tensor orientations relative to the *g*-frame of [$\varphi = 0$, $\theta = \pm 25°$ $\psi = \pm 10°$].[52] If, for simplicity, we ignore the small rotation, ψ,[53] then the data permits two *relative* orientations of **A1**/**T1** and **A2**/**T2**: coaxial (Figure S1 A) and **A1**/**T1** rotated relative to **A2**/**T2** by $\theta = 50°$ (Figure S1 B). In any case, the unit vector along the nearly zero component of **T** (denoted e_2) of H1 is orthogonal to that of H2.

In a second scenario, "B", the patterns of ^{1}H1 and ^{1}H2 do not "cross" at intermediate fields: $A1(g_1) > A2(g_1)$ and $A1(g_3) > A2(g_3)$. The best simulation of the 2D pattern with this scenario, Figure S2, is obtained as the overlap of signals from two $H^{+/-}$, with hyperfine tensors that again both have large isotropic components, $A_{iso} = 24.7$, 21.7 MHz for H1 and H2, respectively, but have noticeably different anisotropic components: **T** for ^{1}H1 is roughly axial, $\mathbf{T} \approx [t, -2t, t]$, where $2t =$ 18.6 MHz; and **T** for ^{1}H2 again is largely rhombic, Table 1. However, the registry of observed and calculated features in the overlap spectra generated in this scenario, Figure S2, is substantially poorer than that of scenario A. Therefore the focus of interpretation will be on scenario A, with little further reference to B.

Discussion

We have reported the preparation and enzymatic properties of the α-70^{Ile} MoFe protein,[27] and have now trapped and characterized by ^{1,2}H ENDOR spectroscopy a remarkable intermediate with two $H^{+/-}$ bound in a *chemically equivalent* manner to the FeMo-cofactor during H^+ reduction. Surprisingly, it is more challenging to deduce the binding mode for these two ^{1}H through ENDOR studies than it was to define that of allyl alcohol,[18] partly because there is less background data on model compounds, and partly because we have no a priori knowledge about the proximity of the two ^{1}H. As the intermediate formed during proton reduction is EPR-active ($S = {}^1/_2$), it must have acquired an even number of electrons during turnover with respect to the resting state ($S = {}^3/_2$) and thus at least has accumulated the elements of H_2 (i.e. two electrons and the two protons). In the Thorneley−Lowe kinetic model[54] for nitrogenase catalysis, it is postulated that reduction of the FeMo-cofactor involves proton-coupled electron transfer and that H_2 can be lost from either a doubly reduced (E_2) or quadruply reduced (E_4) state. Given that the turnover sample was prepared under conditions of low electron flux, with the Fe:MoFe protein ratio of only 0.5:1, if the trapped $S = {}^1/_2$ state of the FeMo-cofactor under study is a true reaction intermediate, it is likely to correspond to the E_2 state.

Why does the cofactor of the α-70^{Ile} MoFe protein accumulate two electrons and two protons, the elements of H_2, without promptly yielding H_2? It is *not* because the amino acid substitution has altered the rate-limiting step for H_2 production: the overall rate of H^+ reduction in this protein is normal. This is consistent with the earlier conclusion that the overall rate-limiting step in the catalytic cycle of nitrogenase is the dissociation of the Fe protein from the MoFe protein at the end of each cycle,[54,55] which is unlikely to be perturbed by the α-70^{Ile} alteration. The buildup of the bound intermediate might reflect either thermodynamic or kinetic consequences of the α-70^{Ile} alteration. In the former case, the α-70^{Ile} substitution might be stabilizing the intermediate state. In the latter case, the α-70^{Ile} substitution may have introduced a kinetic barrier after the formation of this intermediate, thereby allowing its buildup and freeze-trapping. Such a kinetic effect of the α-70^{Ile} substitution might involve alteration of the flux of either H^+ or e^- to the catalytic site, or blocking a subsequent step in the mechanism.

We now discuss structural implications of EPR data for the resting-state of the α-70^{Ile} MoFe protein and of the turnover intermediate. Next, we consider possible sites for the binding of a single $H^{+/-}$ and the characteristics that might be expected of them in an ENDOR experiment. With this foundation, we examine models for the trapped state with two $H^{+/-}$, attempting to find the one(s) that best fit(s) the ENDOR results within the

(50) Mouesca, J. M.; Noodleman, L.; Case, D. A.; Lamotte, B. *Inorg. Chem.* **1995**, *34*, 4347−4359.
(51) Noodleman, L.; Peng, C. Y.; Case, D. A.; Mouesca, J. M. *Coord. Chem. Rev.* **1995**, *144*, 199−244.
(52) Of course, in proper definitions of the Euler angles, negative values of θ are not valid, and are used here for clarity; the proper equivalent Euler rotations involve multiple angles.
(53) Not necessary for simulations.
(54) Thorneley, R. N. F.; Lowe, D. J. In *Molybdenum Enzymes*; Spiro, T. G., Ed.; Wiley-Interscience: New York, 1985; Vol. 7, pp 89−116.
(55) Hageman, R. V.; Burris, R. H. *Proc. Natl. Acad. Sci. U.S.A.* **1978**, *75*, 2699−2702.

Table 2. **g** Tensor Components of Nitrogenase Intermediates under Turnover Conditions with Substrate/Inhibitor

substrate/ inhibitor	MoFe proteins[a]	**g** tensor	refs
CO	WT (lo-CO)	2.09, 1.97, 1.93	59
	WT (hi-CO)	2.17, 2.06, 2.06	
CS_2	WT (a)	2.035, 1.982, 1.973	45
	WT (b)	2.111, 2.022, 1.956	
	WT (c)	2.211, 1.996, 1.978	
C_2H_2	α−195^{Gln}	2.12, 1.98, 1.95	49
$HC{\equiv}CCH_2OH$	α−70^{Ala}	2.123, 1.998, 1.986	25
H^+	α−70^{Ile}	2.14, 2.00, 1.96	current work

[a] The label in parentheses indicates a specific intermediate state among the multiple states generated during the turnover states.

context of the biochemical data. For convenience, the ENDOR results presented above are summarized in the Supporting Information. Finally, we consider some implications of these findings for the catalytic mechanism of nitrogenase.

EPR Spectra of Trapped States. The substitution of Ile for Val at position α-70 in the MoFe protein results in a slight alteration of the resting state FeMo-cofactor EPR spectrum (Figure 2, trace 3). The spectrum has two overlapping $S = {}^3/_2$ signals from two sub-states in which the paramagnetic center differs in rhombicity. The observation of two different sub-states in the resting state is likely to be due to the presence of two major conformations of the larger Ile side chain, *slightly* altering the electronic nature of the EPR center. Similar changes to the $g \approx 3.5-4.5$ region of the EPR spectra of the resting state have been observed with the addition of the substrate C_2H_2 or the inhibitor $C{\equiv}N^-$ to the wild-type MoFe protein[56] and the MoFe protein having altered amino acids at α-96^{Arg}, a residue very near α-70^{Val}.[57] Likewise, similar variations have been seen in the resting-state EPR spectrum of the α-277^{His} MoFe protein variant where His has been substituted for Arg.[58]

When the α-70^{Ile} MoFe protein is trapped during reduction of H^+ to H_2, we observe the EPR spectrum of a novel $S = {}^1/_2$ state (Figure 2, trace 4). Earlier studies on wild-type and altered MoFe proteins also trapped $S = {}^1/_2$ intermediates during turnover with substrates or inhibitors such as CO, CS_2, C_2H_2, or propargyl alcohol.[25,45,49,59] These intermediates all have EPR signals in the $g \approx 2$ region and have similar, but not identical, **g** tensors (Table 2).

Modes of Individual Proton/Hydride Binding to the FeMo-Cofactor. The FeMo-cofactor presents at least five types of $H^{+/-}$ binding mode that must be considered, as presented in Figure 8: (a) terminal hydride bound to an Fe of the face, (b) hydride bound to the terminal Mo, (c) proton bound to a μ^2-bridging sulfide, (d) proton bound to a μ^3-bridging sulfide, and (e) μ^2-hydride bridging two Fe ions within the face. We here describe what little is known and what might be expected for the hyperfine interaction of each of these modes. We then consider how these modes might be combined in the intermediate,[60] as well as models in which H1 and H2 bind to the same site.

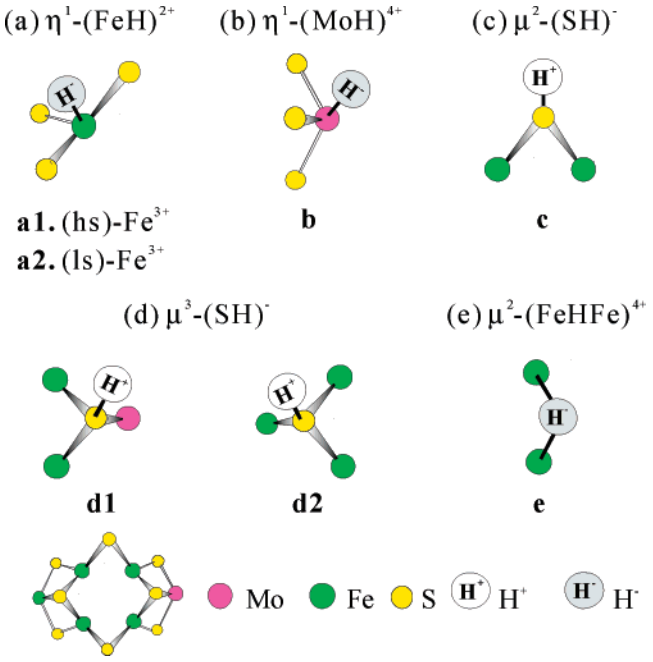

Figure 8. Possible modes of a proton/hydride binding to the FeMo-cofactor. (a) Terminal hydride bound to an Fe, (b) a hydride bound to the terminal Mo, (c) a proton bound to a μ^2-bridging sulfide, (d) a proton bound to a μ^3-bridging sulfide, (e) a μ^2-hydride bridging two Fe ions.

(a) Terminal Hydride at Fe. The only paramagnetic terminal M−H that has been studied, to our knowledge, is H−Co(CO)$_4$ ($S = {}^1/_2$).[61−63] The odd electron of the Co^0(d^9) is in the d_{z^2} orbital; H^- lies along the *z*-axis and has large isotropic and small axial anisotropic components. If the hydride were to be bound with similar covalency, to a high-spin ion (*S*), the isotropic term would be reduced by the factor $(2S)^{-1}$ [64] while the anisotropic term would not,[65] and thus the relative magnitudes of the two contributions could be in line with what we observe. However, the symmetry of **T** would not. The anisotropic ^{1}H coupling for H^- bound to a trigonal (Fe^{3+}-H^-) site of the cofactor would depend on whether the Fe ion is high-spin, Figure 8, a1, or low-spin, Figure 8, a2. A high-spin Fe^{3+} has a spherically symmetric spin distribution and **T** would be axial, unlike the rhombic ^{1}H couplings of *Scenario A*. If Fe^{3+} is low-spin ($S = {}^1/_2$), **T** would depend on the orbital occupied by the single "electron−hole". If the hole spin is in $d_{x^2-y^2}$, d_{xy} or d_{z^2}, and thus **T** would be axial and not in agreement with the analysis of scenario A. For the hole spin in d_{xz} or d_{yz}, **T** would not be precisely axial, but formulas given by Snetsinger and Chasteen[66,67] show that the ^{1}H anisotropic coupling of this case for the appropriate Fe−H^- distance of ≥1.2 Å would be roughly axial. This is borne out by computations for the hydride bound to the Ni−Fe binuclear center of Ni−Fe hydrogenase,[68] although

(56) McLean, P. A.; True, A.; Nelson, M. J.; Lee, H. I.; Hoffman, B. M.; Orme-Johnson, W. H. *J. Inorg. Biochem.* **2003**, *93*, 18−32.
(57) Benton, P. M.; Mayer, S. M.; Shao, J.; Hoffman, B. M.; Dean, D. R.; Seefeldt, L. C. *Biochemistry* **2001**, *40*, 13816−13825.
(58) Shen, J.; Dean, D. R.; Newton, W. E. *Biochemistry* **1997**, *36*, 4884−4894.
(59) Lee, H.-I.; Cameron, L. M.; Hales, B. J.; Hoffman, B. M. *J. Am. Chem. Soc.* **1997**, *119*, 10121−10126.
(60) We note that the two distinguishable, although chemically equivalent, protons detected by ENDOR spectroscopy necessarily represent two distinct proton-binding sites, but the data do not preclude the possibility that we are studying two populations of intermediate, each with a single 1H bound.
(61) Fairhurst, S. A.; Morton, J. R.; Preston, K. F. *J. Magn. Reson.* **1983**, *55*, 453−459.
(62) Poli, R. In *Recent Advances in Hydride Chemistry*; Peruzzini, M., Poli, R., Eds.; Elsevier Science B. V.: Amsterdam, Netherlands, 2001; pp 139−188.
(63) A Mo-trihydride has been studied by Poli and co-workers.
(64) Atherton, N. M. *Principles of Electron Spin Resonance*; Ellis Horwood: New York, 1993.
(65) Hutchison, C. A., Jr.; McKay, D. B. *J. Chem. Phys.* **1977**, *66*, 3311−3330.
(66) Snetsinger, P. A.; Chasteen, N. D.; van Willigen, H. *J. Am. Chem. Soc.* **1990**, *112*, 8155−8160.
(67) Our computations employ minor corrections supplied by Prof. Chasteen.
(68) Brecht, M.; van Gastel, M.; Buhrke, T.; Friedrich, B.; Lubitz, W. *J. Am. Chem. Soc.* **2003**, *125*, 13075−13083.

the experimental tensor is more rhombic than the calculated one.[69] Therefore, it is unlikely that either a high- or low-spin terminal ($Fe^{3+}-H^-$) would give rise to the ^1H hyperfine tensors determined with the analysis of Scenario A.

(b) Terminal Hydride at Mo. An η^1-terminal hydride bound to the Mo ion, (Mo^{5+}-H^-), Figure 8 b, would have a d^1 configuration. Again, the ^1H tensor would depend on the orbital bearing this electron, but it would be expected that **T** would be axial or largely so. Hence, this mode of binding also does not appear to suit the observed ^1H tensor of Scenario A.

(c) Protonated Sulfide. Protonation of a μ^2-$(S)^{2-}$ to form a [Fe−$(SH)^-$−Fe] fragment at the cluster waist is chemically attractive (Figure 8 c). Although we know of no case where an $[Fe_nS_m]$ cluster actually binds protons when at least one Fe ion is in the ferric state, many model compounds with two metal ions bridged by one or more $(SH)^-$ are known (Figure 8 c).[70] Our studies of $S = {}^1/_2$ mixed-valence di-iron centers with antiferromagnetically coupled Fe^{III} ($S = {}^5/_2$) and Fe^{II} ($S = 2$) Fe ions[71,72] show that the proton on a bridging $(OH)^-$ has a rhombic dipolar interaction with the Fe ions, **T**, as seen here, and the formulas that describe the **T** for the proton on a bridging $(XH)^-$ show that **T** for the coupling of a [Fe−$(SH)^-$−Fe] fragment also would be rhombic (see Supporting Information for considerations of the anistropic ^1H hyperfine tensors for protonated μ^2- and μ^3-sulfides). More than counterbalancing these factors, however, the [Fe−(OH)−Fe] proton has negligible isotropic hyperfine coupling, in sharp contrast to the two $H^{+/-}$ seen here. To our knowledge, only one EPR study of paramagnetic [Fe−$(SH)_n$−Fe], $n = 1, 2$, models has been published, by Keizer et al.[73] It also shows small isotropic couplings to the ^1H (∼6 MHz, $n = 1$; ∼4 MHz, $n = 2$) and if the $(SH)^-$ in the cofactor bridges high-spin ions, as is likely (but unlike the model), these values would be further reduced by $(2S)^{-1}$ factors. In addition, we note that the spin densities on the X^{2-} of the $[Fe_2\text{-}Se_2]^+$ cluster (X = Se) reconstituted into a ferredoxin,[74] of the $[Fe_4\text{-}S_4]^+$ cluster (X = S) of aconitase, [75] and of the resting-state Fe−Mo cofactor[76] all have small hyperfine couplings to X and, hence, small net spin densities, just as with hydroxo and oxo bridges in the hydroxo-bridged diiron centers. Thus, [Fe−$(SH)^-$−Fe] is not likely to yield the observed large ^1H isotropic coupling, and we currently disfavor such an assignment for H1 or H2; studies of model compounds will test this inference. Note that this objection applies to *both* scenarios for the interpretation of the 2D ENDOR plots.

(d) Bridging Hydrides. Numerous M−$(H)_n$−M model structures (Figure 8 e), are known,[77−83] but only the $S = {}^1/_2$ [Fe−$(H)_n$−Fe], $n = 1, 2$, paramagnetic model compounds of Keizer et al.[73] provide any background information for our analysis. The isotropic couplings for the bridging ^1H are large and could fall into the range observed when diminished by the $(2S)^{-1}$ factors for a bridge between high-spin ions (see above). Calculations for **T** based on the likely geometry of such a fragment as incorporated into the analytical formula for H^- bridging two high-spin Fe ions[71] suggest that the observed rhombic **T** could be achieved by a bridging hydride at the appropriate Fe−H distances (∼1.5−1.6 Å) from nonpoint-dipole Fe spins.[66] Thus, we consider this to be a potentially viable model for interpretation of the ENDOR data. The principal-axis directions of **T** have the same characteristics as for bridging $(SH)^-$ (see Supporting Information).

Models for the $S = {}^1/_2$ Turnover-Intermediate State with Two Bound Protons/Hydrides. The two ^1H hyperfine tensors for the $S = {}^1/_2$ trapped state have the same principal values, according to the preferred interpretation of the ENDOR data, scenario A, and from this we have inferred that the two $H^{+/-}$ are bound in a chemically equivalent fashion. As displayed in eq 3, the **A** tensor for a bound ^1H depends not only on its chemical environment, as manifested in the hyperfine interactions, A_i, but also on the spin-coupling coefficients of the cluster metal ions, K_i. In the following discussions we disfavor models which would require "accidental" equivalence of spin-coupling parameters that are not intrinsically correlated. In particular, we discuss only models with two hydrogenic species of the same type.

(i) Models with Two Protonated Sulfides. We argue above that a protonated sulfide would not have a sufficiently large value of A_{iso} to match the experimentally derived values for H1 and H2. Additional considerations lead us to further disfavor models (Figure 9 A) for the cluster state with two equivalent protonated sulfides: in order for $^1H1$ and $^1H2$ of two [Fe−$(SH)^-$−Fe] units to have the same, rhombic, dipolar couplings would require that the iron ions fortuitously have the same *pair* of vector-coupling coefficients; tensor orientations also present a difficulty, as discussed in the Supporting Information.

(ii) Hydride Models. The above discussions of the hyperfine tensor for such a model suggest that any state with two terminal hydrides is unlikely, as neither ($Fe^{3+}-H^-$) nor ($Mo^{5+}-H^-$) is expected to have the observed rhombic hyperfine tensor. In addition, for such an assignment to give identical principal values for H1 and H2, the two metal ions would be required to fortuitously have the same vector-coupling coefficients. Thus, models **B1** and **B2** (Figure 9), with two such moieties, are disfavored.

Models in which two hydrides (**B3** in Figure 9) bridge two pairs of Fe ions at the waist (**B3a** and **B3b** in Figure S4) or three connected Fe ions (**B3c** and **B3d** in Figure S4) appear capable of exhibiting the hyperfine tensors we have measured, provided that the two pairs of Fe ions in **B3a** and **B3b**, or the

(69) Foerster, S.; Stein, M.; Brecht, M.; Ogata, H.; Higuchi, Y.; Lubitz, W. *J. Am. Chem. Soc.* **2003**, *125*, 83−93.
(70) Leggate, E. J.; Bill, E.; Essigke, T.; Ullmann, G. M.; Hirst, J. *Proc. Natl. Acad. Sci. U.S.A.* **2004**, *101*, 10913−10918.
(71) DeRose, V. J.; Liu, K. E.; Lippard, S. J.; Hoffman, B. M. *J. Am. Chem. Soc.* **1996**, *118*, 121−134.
(72) Smoukov, S. K.; Quaroni, L.; Wang, X.; Doan, P. E.; Hoffman, B. M.; Que, L., Jr. *J. Am. Chem. Soc.* **2002**, *124*, 2595−2603.
(73) Keizer, P. N.; Krusic, P. J.; Morton, J. R.; Preston, K. F. *J. Am. Chem. Soc.* **1991**, *113*, 5454−5456.
(74) Orme-Johnson, W. H.; Hansen, R. E.; Beinert, H.; Tsibris, J. C.; Bartholomaus, R. C.; Gunsalus, I. C. *Proc. Natl. Acad. Sci. U.S.A.* **1968**, *60*, 368−372.
(75) Werst, M. M.; Kennedy, M. C.; Houseman, A. L. P.; Beinert, H.; Hoffman, B. M. *Biochemistry* **1990**, *29*, 10533−10540.
(76) Venters, R. A.; Nelson, M. J.; McLean, P. A.; True, A. E.; Levy, M. A.; Hoffman, B. M.; Orme-Johnson, W. H. *J. Am. Chem. Soc.* **1986**, *108*, 3487−3498.
(77) Ohki, Y.; Suzuki, H. *Angew. Chem., Int. Ed.* **2000**, *39*, 3120−3122.
(78) Bazhenova, T. A.; Kachapina, L. M.; Shilov, A. E.; Antipin, M. Y.; Struchkov, Y. T. *J. Organomet. Chem.* **1992**, *428*, 107−123.
(79) Bottcher, H. C.; Graf, M.; Merzweiler, K.; Wagner, C. *J. Org. Chem.* **2001**, *628*, 144−150.
(80) Boncella, J. M.; Green, M. L. H. *J. Org. Chem.* **1987**, *52*, 217−231.
(81) Ohki, Y.; Kojima, T.; Oshima, M.; Suzuki, H. *Organometallics* **2001**, *20*, 2654−2656.
(82) Boncella, J. M.; Green, M. L. H.; Ohare, D. *J. Chem. Soc., Chem. Commnun.* **1986**, 618−619.
(83) Dapporto, P.; Midollini, S.; Sacconi, L. *Inorg. Chem. Commun.* **1975**, *14*, 1643−1650.

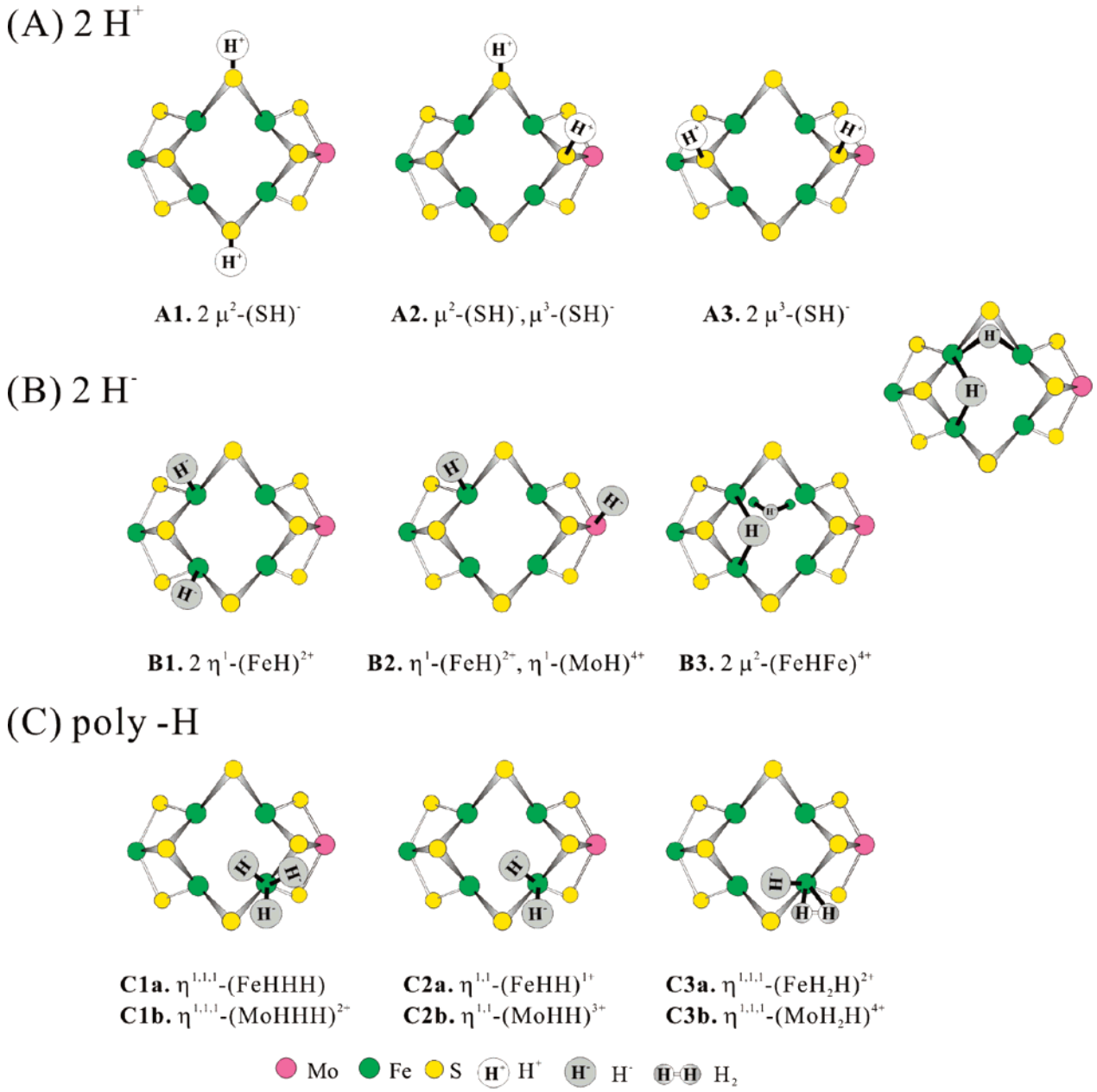

Figure 9. Models for the α-70^{Ile} MoFe protein turnover intermediate state. (A) models with two protonated sulfurs, (B) models with two hydrides, and (C) models with poly-hydrogenic species bound to Fe. In **B3**, smaller bridging hydride represents second bridging hydride. See Figure S4.

"first" and "third" of the three Fe ions in **B3c** and **B3d**, have the same vector-coupling coefficients. As it is possible that the hydride bridges "induce" the proper spin-coupling scheme, we believe that this model warrants further consideration. We nonetheless note that models with bridging hydrides do not appear to satisfy the experimentally derived relative orientations of the hyperfine tensor for the two H^- (Figure S3 A−C); the arguments are similar to those presented regarding the orientation of **T** for an [Fe−(SH)$^-$−Fe] site (Supporting Information). An alternate version of this model, with *two* hydrides bridging the same pair of Fe ions (**B3e** in Figure S4), eliminates the problem of "accidental" equality of *K*'s, but it is even less likely that this model could give the correct relative orientations of H1 and H2 for the observed tensors (Figure S3 A).

An obvious way to avoid having to propose what might be serendipitous values of spin-coupling coefficients on several Fe ions, or pairs of Fe ions, is for ^{1}H1 and ^{1}H2 to be bound to a single metal ion. For Mo to form a di(or tri-)-hydride, or dihydrogen-hydride (**C1b**, **C2b**, and **C3b** in Figure 9) it would need to lose not one, but two (or three) of the resting-state ligands or expand its coordination sphere. Examination of Fe model structures discloses three such models for consideration: Fe-trihydride (**C1a** in Figure 9), Fe-dihydride (**C2a)**, and Fe-dihydrogen-hydride (**C3a)**.

Trihydrides of Fe (and Mo)[62,84] (**C1a**) are well-known and would provide a natural way to generate hyperfine tensors related by a three-fold axis. If such a center were present, the reduction state of the MoFe protein would presumably be E_4 and not E_2. Three hydrides bound to a waist Fe of the FeMo-factor would have a six-coordinate pseudo-octahedral geometry

(84) Pleune, B.; Morales, D.; Meunier-Prest, R.; Richard, P.; Collange, E.; Fettinger, J. C.; Poli, R. *J. Am. Chem. Soc.* **1999**, *121*, 2209−2225.

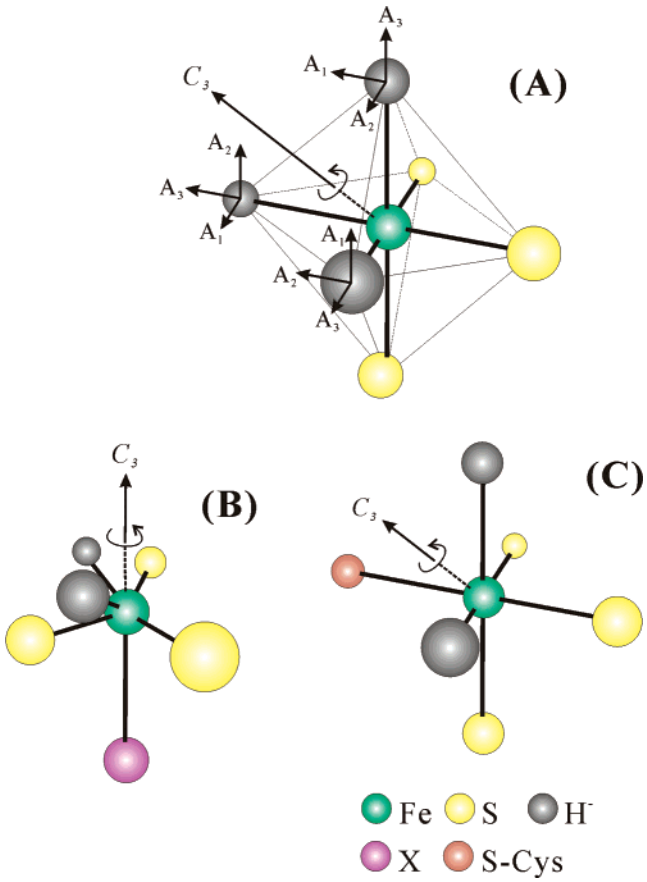

Figure 10. Binding models of hydrides to a single Fe ion with pseudo-octahedral geometry. (A) Idealized model with facial-trihydride in an octahedron satisfying permuting of ^{1}H hyperfine tensors, (B) model with dihydride on a waist Fe, and (C) model with dihydride on the terminal Fe.

by releasing its bond to X, then the hydrides would be related by a 120° rotation about the pseudo-trigonal axis through the hydride face, as illustrated in Figure 10 A. This symmetry element would permute the hyperfine components in a coaxial fashion as observed in the scenario A simulation of the experimental results. Likewise, the angle between the unit vectors along the intermediate tensor components (e_2) for H1 and H2 is near to 90° (also a requirement of the other two possible orientations).

Unfortunately, to explain the observation of signals from only two types of ^{1}H, this model requires two hydrides of the three to be magnetically indistinguishable, so that these two together give rise to one of the two ^{1}H signals detected. This is possible only if the indistinguishable hydrides occupy positions that are mirror-equivalent with respect to a plane of the **g** tensor framework. However, the combination of relative orientations between the hyperfine tensors and their absolute orientations with respect to the **g** tensor frame appears to make this impossible: this equivalence would require that the hyperfine frames make angles of 45° with respect to an axis plane (g_1-g_2, etc.) of the **g** tensor, contrary to experiment.

Another structure with three hydrogenic species bound on one Fe; a dihydrogen-hydride (**C3c** in Figure 9) also is well-known.[85,86] In these structures, the dihydrogen typically binds quite unsymmetrically, with the hydride 90° away. However, we cannot see how such a structure could give ENDOR patterns associated with two ^{1}H that appear to be chemically equivalent (equal hyperfine tensor components).

A six-coordinate pseudo-octahedral geometry might obtain if a waist Fe were to bind two hydrides and *retain* its bond to X, e.g., Figure 10 B. Alternatively, the terminal Fe (Fe1) might achieve such a geometry simply by adding the two hydrides, Figure 10 C. A di-hydride at a terminal Fe might be compatible with the fact that the intermediate occurs only in the presence of a mutation above the 4Fe face, if the intermediate builds up because of a kinetic barrier after its formation, as discussed above. Unfortunately there is no information from model compounds about the hyperfine tensor expected for such centers, and it is *not* obvious that such centers could accommodate the rhombic **T** of H1 and H2.

For completeness, we note that the assignment of the two nonequivalent hydrides implied by scenario B, which we do not favor, would be rather straightforward. In this scenario, H1 has an axial tensor and is assignable as a terminal hydride, while H2 has a roughly rhombic tensor, and would be assignable as a bridging hydride.

Summary

The α-70^{Ile} MoFe protein shows undiminished ability to reduce H^+ but is severely compromised in the reduction of acetylenic compounds and N_2. These observations support the proposal that both acetylenic compounds and N_2 are reduced at the Fe-2, -3, -6, -7 face of FeMo-cofactor. We here report that the FeMo-cofactor of the α-70^{Ile} MoFe protein converts to an $S = {}^1/_2$, EPR-active state during H^+ reduction/H_2 evolution. This intermediate state has been freeze-trapped and characterized by ^{1,2}H ENDOR spectroscopy. The ENDOR spectra show that the turnover MoFe protein binds two $H^{+/-}$. This finding is consistent with an assignment of the intermediate as the E_2 state formed during the reduction of nitrogen, a state in which the cofactor has accumulated the elements of H_2; however, this remains to be established.

The hyperfine tensors of the two $H^{+/-}$ have been determined from 2D field-frequency plots of ^{1}H ENDOR spectra collected across the EPR envelope of the intermediate. The tensors have large isotropic components, which shows that the two $H^{+/-}$ are covalently bound to the $S = {}^1/_2$ cofactor cluster. In the favored analysis for these *2*D plots (Figure 7 and Table 1), the principal values of the hyperfine tensors of the two $H^{+/-}$ are the same, within error, indicating that the two bound $H^{+/-}$ are *chemically equivalent*. The two $H^{+/-}$ are not symmetry-equivalent, as they give distinct ENDOR signals, but the tensors are related to each other by a permutation of the tensor components, which must reflect an underlying symmetry of binding relative to the cofactor.

The observed hyperfine tensors for H1 and H2 have been compared with those expected for various potential modes of $H^{+/-}$ binding to the cofactor, based on limited data from reference/model complexes. At present, no model for the structure of the cofactor in the $S = {}^1/_2$ state trapped during reduction of H^+ can be shown unequivocally to satisfy all of the constraints generated by the ENDOR analysis, as sum-

(85) Gusev, D. G.; Hubener, R.; Burger, P.; Orama, O.; Berke, H. *J. Am. Chem. Soc.* **1997**, *119*, 3716−3731.

(86) Vandersluys, L. S.; Eckert, J.; Eisenstein, O.; Hall, J. H.; Huffman, J. C.; Jackson, S. A.; Koetzle, T. F.; Kubas, G. J.; Vergamini, P. J.; Caulton, K. G. *J. Am. Chem. Soc.* **1990**, *112*, 4831−4841.

marized in the Supporting Information. Nonetheless, the analysis disfavors any model that involves protonation of sulfide(s). We make this inference while recognizing that the few computations that address proton-binding intermediates tend to favor protonated sulfide;[13,51,87] new computations which address our ENDOR constraints will be required. The analysis thus suggests that the intermediate instead contains two chemically equivalent bound hydrides, which are unlikely to be terminal monohydrides. Two models for the binding of H1 and H2 seem worthy of additional consideration: an Fe-dihydride formed on an Fe of the Fe-2, -3, -6, -7 face (Figure 10 C), two hydrides bridging Fe ions (**B3** in Figure 9 and Figure S4). Our suggestion that hydrides bind to Fe in this trapped intermediate does not preclude the possibility that H^+/H^- exhibit different modes of binding to the FeMo-cofactor in other reaction steps or reduction states.

These current studies will be extended by further ENDOR experiments, not only studies of the enzyme but also of newly emerging model compounds,[20,23] and the problem will be explored by new computations. In principle, hydrides might also be detected, or ruled out, by infrared spectroscopy.[88] Efforts to establish the mode of binding for nitrogenous intermediates related to nitrogen reduction also are under way in our laboratories.

Acknowledgment. We thank Dr. Brett Barney for assistance with EPR data collection. This work was supported by the NSF (MCB-0316038 to B.M.H.), the NIH (GM-59087 to L.C.S. and D.R.D. and HL13531 to B.M.H.), and the Korea Research Foundation (KRF-2003-070-C00029 to H.I.L.).

Supporting Information Available: Text plus four figures. This material is available free of charge via the Internet at http://pubs.acs.org.

JA043596P

(87) Durrant, M. C. *Biochemistry* **2002**, *41*, 13946−13955.
(88) Thorneley, R. N. F.; George, S. In *Prokaryotic Nitrogen Fixation*; Triplett, E. W., Ed.; Horizon Scientific Press: Norfolk, England, 2000; pp 1−14.